Supporting Information

Selectively disrupting m^{6}A-dependent protein-RNA interactions with fragments

Rajiv Kumar Bedi[1], Danzhi Huang[1], Lars Wiedmer[1], Yaozong Li[1], Aymeric Dolbois[1], Justyna Aleksandra Wojdyla[2], May Elizabeth Sharpe[2], Amedeo Caflisch[1*], Pawel Sledz[1*]

[1] Department of Biochemistry, University of Zurich, Winterthurerstrasse 190, CH-8057 Zurich, Switzerland

[2] Swiss Light Source, Paul Scherrer Institute, Villigen, Switzerland

[*] To whom correspondence should be addressed. Amedeo Caflisch; Email: caflisch@bioc.uzh.ch, Paweł Śledź; Email: p.sledz@bioc.uzh.ch

Material and methods

Protocols for protein purification, crystallization, diffraction data collection and refinement of the YTHDC1-ligand complexes were reported previously.[1]

Protein purification

The plasmid expressing the N-terminally hexahistidine-tagged YTH domain (residues 345-509) of human YTHDC1 protein was a gift from Cheryl Arrowsmith (Addgene ID: 64652). The recombinant protein was purified to homogeneity in two chromatographic steps. The protein was overexpressed for 16 hours at 24°C in *Escherichia coli* BL21 (DE3) cells upon induction with 0.4 mM IPTG. The cells were harvested and resuspended in the lysis buffer containing 100 mM Tris-HCl at pH 8.0, 500 mM NaCl and 10 mM imidazole. The cells were lysed by sonication and the cell lysate was clarified by centrifugation at 48,000 g for one hour and loaded onto Ni-NTA affinity column (5 mL HisTrap FF from GE Healthcare). After extensive washing with the wash buffer containing 100 mM Tris-HCl at pH 8.0, 500 mM NaCl and 50 mM imidazole the target protein was eluted with elution buffer containing 100 mM Tris-HCl at pH 8.0, 500 mM NaCl and 250 mM imidazole. The N-terminal hexahistidine-tag was removed by cleavage with tobacco etch virus (TEV) protease at 1:50 ratio. The excess imidazole was removed by overnight dialysis and the sample was subjected to secondary subtractive Ni-NTA affinity chromatography step to remove the protease and uncleaved protein. Finally, the protein was subjected to a gel filtration step using Superdex 75 16/60 column in a buffer containing 10 mM Tris-HCl at pH 7.5, 150 mM NaCl and 1 mM DTT. The protein was concentrated to 10 mg/mL, flash-frozen in liquid nitrogen and stored at -80 °C for future experiments.

Crystallography

The crystals of YTHDC1 YTH domain were obtained by mixing 1 µL protein solution at 10 mg/mL with mother liquor containing 0.1 M Bis-Tris at pH 6.5, 0.2 M ammonium sulfate and 25% PEG 3350 at 22°C in a hanging drop vapor diffusion setup. To obtain crystals of protein complexed with fragments, the crystals were transferred to a 1 µL drop containing 50-200 mM (depending on the solubility) fragment directly dissolved in 0.1 M Bis-Tris at pH 6.5, 0.2 M ammonium sulfate and 30% PEG 3350, soaked overnight at 22 °C, harvested and frozen in liquid nitrogen without additional cryoprotection.

Diffraction data were collected at the Swiss Light Source (Villigen, Switzerland) using the beamline X06DA (PXIII), and processed using XDS.[2] The structures were solved by molecular replacement using Phaser program[3] from the Phenix package.[4] The unliganded structure of YTHDC1 (PDB ID: 4R3H) was used as a search model. The model building and refinements were performed using COOT[5] and phenix.refine.[6] Data collection and refinement statistics are summarized in Table S1.

IC_{50} value determination on YTHDC1

The IC_{50} value for each fragment was measured by a competition binding assay where the test compound competes with m^6A-containing oligoribonucleotide for the m^6A binding site of YTHDC1. The binding of the 5'-biotinylated single-stranded oligoribonucleotide (5'-AAGAACCGGm^6ACUAAGCU-3') to recombinant GST-tagged YTH domain of the YTHDC1 protein (residues 345-509) was assessed by homogeneous time-resolved fluorescence (HTRF) as proposed previously as detection system in the reader-based assay for m^6A writer/eraser enzymatic activity.[7] The signal is reduced when a test compound displaces the m^6A-containing oligoribonucleotide from the complex. The assay was performed in a total volume of 20 µl in a white 384-well microplate (Corning, 4513). All the reagents, except the compounds, were prepared in the assay buffer (50 mM HEPES, pH 7.5, 150 mM NaCl, 100 mM KF, and 0.1% (m/v) bovine serum albumin). Compounds dissolved in DMSO were incubated with GST-tagged YTHDC1 and biotinylated

m^{6}A-containing oligoribonucleotide at room temperature for 10 minutes. Subsequently, the HTRF reagents, anti-GST Eu^{3+}-labelled antibody (Cisbio, 61GSTKLB) and XL665-conjugated streptavidin (Cisbio, 610SAXLB), were added. The final assay buffer contained 10% (v/v) DMSO, 25 nM GST-tagged YTHDC1, 16 nM 5'-biotinylated m^{6}A-containing ribonucleotide, 0.8 nM anti-GST Eu^{3+}-labelled antibody and 2 nM XL665-conjugated streptavidin. The reaction was allowed to equilibrate at room temperature for 3 hours. Infinite M1000 plate reader (Tecan) recorded with a delay of 60 µs the emission at 620 and 665 nm, after the excitation of the anti-GST Eu^{3+}-labelled antibody at 317 nm. The IC_{50} values derived from fitting a dose-response curve to the data using the non-linear regression analysis in GraphPad Prism version 8.0.

Selectivity screening against YTHDF1/2/3

The assay applied for the selectivity screening of the fragments against YTHDF1/2/3 was based on the described HTRF method for YTHDC1 above. Briefly, the fragments were first incubated with the GST-tagged YTH domain and biotinylated m^{6}A-containing oligoribonucleotide (5'-AAGAACCGGm^{6}ACUAAGCU-3') at room temperature for 10 min. Subsequently, the HTRF reagents were added and after 3 hours of incubation the HTRF signal was measured as described above. All three assays were carried out the same, such that the final assay buffer (50 mM HEPES, pH 7.5, 150 mM NaCl, 100 mM KF, and 0.1% (m/v) bovine serum albumin) contained 1% (v/v) DMSO, 25 nM GST-tagged YTH domain ($YTHDF1_{361-559}$, $YTHDF2_{383-579}$, $YTHDF3_{391-585}$), 15 nM 5'-biotinylated m^{6}A-containing ribonucleotide, 0.8 nM anti-GST Eu3+-labelled antibody and 1.8 nM XL665-conjugated streptavidin.

Isothermal titration calorimetry (ITC)

The ITC measurements were carried out using MicroCal ITC200 (GE Healthcare) as previously described.[1] In brief, test compounds were dissolved at the final concentration of 1-10 mM in the buffer containing 20 mM HEPES, pH 7.5 and 150 mM NaCl, and titrated in 16 injections of 2.5 µl into the sample cell containing recombinant YTHDC1 at a concentration of 60 µM. Data were fitted to the single binding site model provided in the MicroCal Origin software package.

Molecular dynamics simulations and binding pocket analysis

The apo structure for MD simulations was prepared based on the structure of the YTH domain of YTHDC1 complexed with a m^{6}A-containing oligoribonucleotide (PDB ID: 4R3I)[8] by removing the oligomer. The hydrogen atoms were added by the CHARMM program[9] and the protonation states were determined at neutral pH conditions. The apo structure were solvated in a 66 Å of rhombic dodecahedron TIP3P water box[10] to ensure 10 Å buffer layer between the protein atoms and the boundary of the water box. Na^+ and Cl^- ions at 0.15 M concentration were added to neutralize the system. The CHARMM36 force field was used to describe the protein physics.[11]

The simulation system was minimized for 10,000 steps under a series of restraints and constraints on the protein atoms to release its unfavourable contacts and fix its poor geometry. The minimized structure was then heated to 300 K and equilibrated in NVT condition (constant volume and temperature). Finally, the structure was further equilibrated in NPT condition (constant pressure and temperature). All the equilibration phases lasted for 1 nanosecond using the CHARMM program (version 42b2).[9] Production MD runs were carried out in NPT conditions using the NAMD program (version 2.12).[12] The pressure was controlled by Nosé-Hoover Langevin piston method with 200 picoseconds piston period and 100 picoseconds piston decay time.[13, 14] The temperature was maintained at 300 K using the Langevin thermostat with a 5 picoseconds friction coefficient. The integration time step was set to 2 femtoseconds by constraining all the bonds involving hydrogen atoms by the SHAKE algorithm. Van der Waals energies were calculated using a switching function with a switching distance from 9 to 11 Å[15], and electrostatic interactions were evaluated using the particle mesh Ewald summation (PME) method.[16] Two independent runs of 1 microsecond each were carried

out with the same equilibrated structure but different initial velocities. MD snapshots were saved every 10 picoseconds along the MD trajectories for further analysis.

The MDpocket routine embedded in the software fpocket (version 3.0)[17, 18] was used to measure the solvent accessible surface area (SASA) of the YTHDC1 binding pocket from MD simulations. First, the reference structure was build based on the holo structure (PDB ID: 4R3I) by removing its bound oligoribonucleotide. All MD snapshots were then superposed onto the reference structure. Second, the alpha sphere centers[18] for describing the m^{6}A binding pocket was then generated. The alpha sphere centers were used for roughly locating the corresponding pocket of all MD snapshots. Finally, SASA values of the dynamic binding pocket were calculated along the MD trajectories guided by the reference alpha sphere centers. Default parameters were applied for the calculations and the SASA values with a probe of 2.2 Å were presented here. We also applied the same parameters to obtain the SASA values for 26 of thirty complex structures released in this study (except fragment **22**, **24**, **26** and **27**).

Figure S1: ITC curves for the fragment **11**, **13**, **26** and m^{6}A. For fragments **11** and **26**, **13**, and m^{6}A, the DMSO was kept at 1%, 10%, and 0%, respectively. The association constant (K_a), enthalpy (ΔH) and entropy (ΔS) are tabulated. The stoichiometry (n) was fixed to 1 in each case due to weak binding.

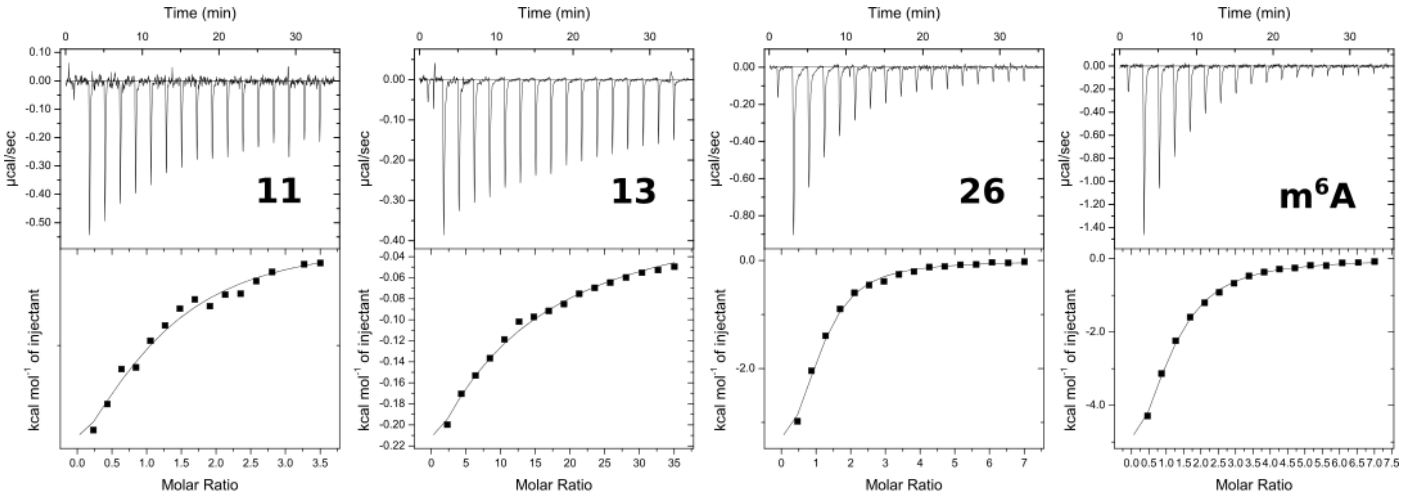

	n	K_a (M^{-1})	ΔH (kcal/mol)	ΔS (cal/mol/deg)
11	1.00	1.71E4 ± 0.2E4	-3.656E3 ± 0.2E3	6.9
13	1.00	4.74E2 ± 0.2E2	-7.6E3 ± 0.2E3	-13.9
26	1.00	4.46E4 ± 0.4E4	-4.496E3 ± 0.1E3	5.9
m^{6}A	1.00	2.78E4 ± 0.1E4	-7.807E3 ± 0.1E3	-6.3

Figure S2: Dose-response curves derived from competitive HTRF assay. Fragments **25** and **28** could not be measured at very high concentrations because of poor solubility. To enable the fitting for these two fragments, an additional data point (in red) was added at 100 mM, with the assumption that complete disruption of binding would be achieved at this concentration. All curves are for YTHDC1 except for the bottom row (red box) which are for fragment **26** and the YTHDF1/2/3 readers.

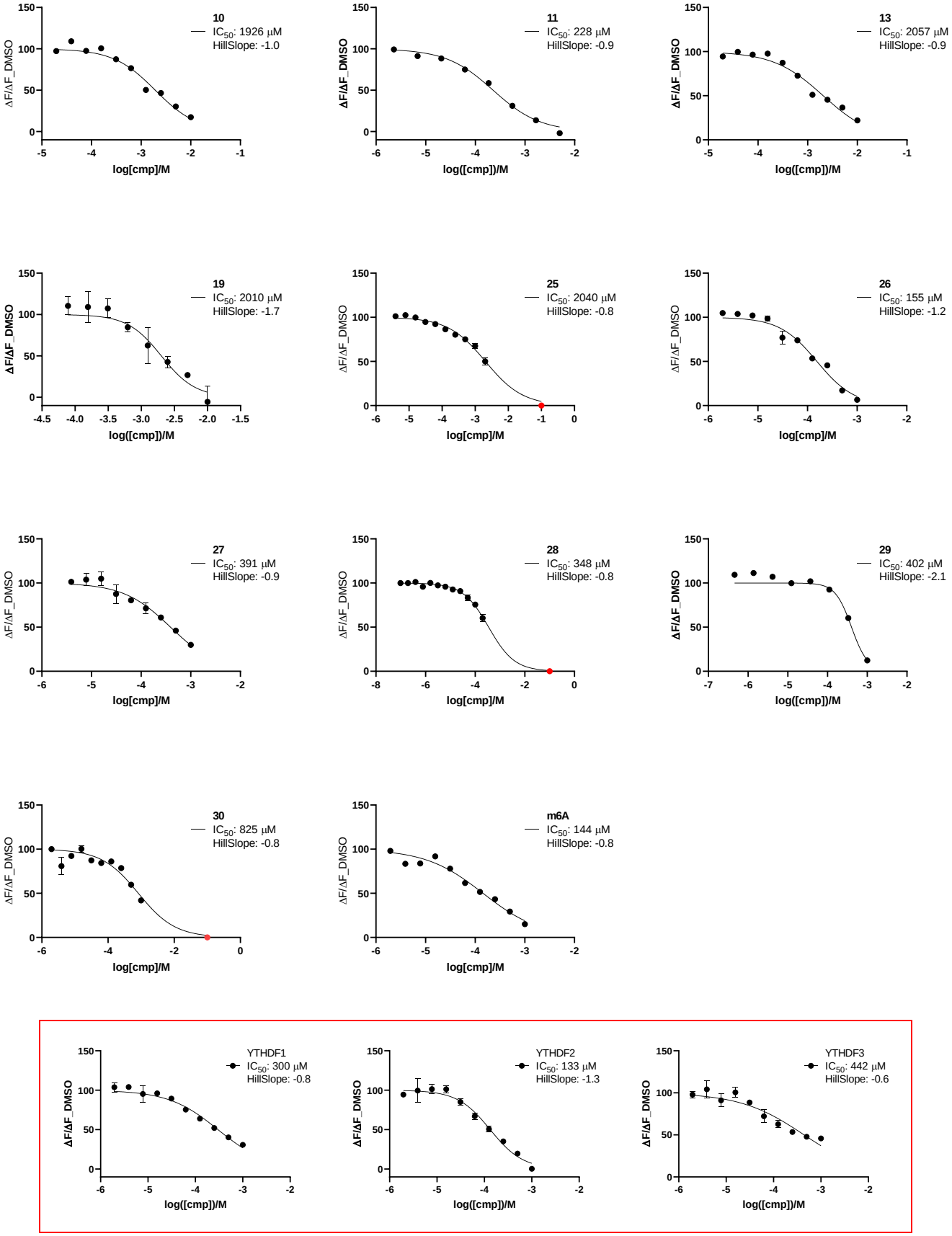

Table S1: PDB codes and X-ray data collection and refinement statistics for complex structures of the YTHDC1 reader domain and fragments.

PDB ID:	6SYZ	6SZ1	6SZ2	6SZ3	6SZ7
Fragment	**1**	**2**	**3**	**4**	**5**
Data Collection					
Space group	$P12_11$	$P12_11$	$P12_11$	$P12_11$	$P12_11$
Cell dimension a, b, c (Å)	39.92, 103.33, 42.29	39.83, 103.35, 42.38	39.92, 103.56, 42.38	39.65, 103.45, 42.22	39.50, 102.99, 42.06
Cell dimension α, β, γ (°)	90, 106.72, 90	90, 107.14, 90	90, 105.46, 90	90, 105.89, 90	90, 105.08, 90
Resolution (Å)	40.49 (2.28)	40.49 (1.74)	40.84 (1.52)	40.61 (1.28)	40.60 (2.28)
Unique reflections*	14467 (2261)	60875 (9342)	94294 (15417)	156810 (24690)	14251 (2198)
Completeness*	98.1 (95.4)	92.7 (88.2)	95.4 (94.2)	94.7 (92)	96 (92.4)
Redundancy*	3.38 (3.49)	1.8 (1.79)	1.76 (1.76)	1.74 (1.71)	3.12 (2.69)
R_{merge}*	4.4 (13.2)	8.8 (106.2)	11.7 (86)	5.5 (108.9)	23.1 (105.2)
CC (1/2)	99.9 (99.1)	99.5 (68.2)	98.6 (61.9)	99.9 (43.2)	97.8 (55.2)
I/σI	24 (9.9)	6.54 (1.02)	4.34 (0.91)	9.06 (0.87)	5.37 (1.11)
Refinement					
R_{work}/R_{free}	0.1760/0.2358	0.2219/0.2671	0.2083/0.2455	0.1942/0.2053	0.1971/0.2651
RMSD bond (Å)	0.007	0.006	0.006	0.005	0.008
RMSD angle (°)	0.828	0.824	0.792	0.786	0.996
B-factor (Å²)**	25.67/35.60/28.91	34.56/42.40/38.82	24.10/32.54/33.07	19.56/28.30/30.79	32.10/41.51/35.28
Ramanchandran Favored	98.15	99.07	98.4	99.37	98.44
Ramanchandran allowed	1.54	0.93	1.6	0.63	0.56
Ramanchandran Disallowed	0.31	0	0	0	0

PDB ID:	6SZ8	6SZL	6SZN	6SZR	6SZT
Fragment	**6**	**7**	**8**	**9**	**10**
Data Collection					
Space group	$P12_11$	$P12_11$	$P12_11$	$P12_11$	$P12_11$
Cell dimension a, b, c (Å)	39.73, 103.62, 42.06	39.68, 103.69, 42.12	39.71, 103.83, 41.99	39.51, 103.29, 41.95	39.72, 103.84, 42.04
Cell dimension α, β, γ (°)	90, 104.19, 90	90, 105.51, 90	90, 104.79, 90	90, 105.39, 90	90,104.49, 90
Resolution (Å)	40.77 (1.46)	40.58 (1.45)	40.59 (1.47)	40.44 (1.64)	40.70 (1.5)
Unique reflections*	54009 (8272)	56386 (8373)	54920 (8115)	39367 (6195)	51724 (8120)
Completeness*	94.9 (90)	96.4 (88.9)	97 (89.2)	99.1 (97.2)	96.9 (94.4)
Redundancy*	3.06 (2.74)	3.32 (2.83)	3.37 (3.14)	3.42 (3.34)	3.25 (2.94)
R_{merge}*	5.9 (60.7)	5.6 (56.2)	6.1 (143)	14 (142)	2.9 (11.5)
CC (1/2)	99.8 (78.4)	99.8 (81.8)	99.8 (43.3)	99.6 (40.5)	99.9 (98.8)
I/σI	11.22 (1.52)	12.44 (2.05)	10.73 (0.9)	8.09 (1.04)	29.24 (11.51)
Refinement					
R_{work}/R_{free}	0.2161/0.2494	0.1928/0.2155	0.1828/0.2184	0.1924/0.2399	0.1753/0.1993
RMSD bond (Å)	0.006	0.006	0.005	0.006	0.005
RMSD angle (°)	0.814	0.790	0.738	0.759	0.790
B-factor (Å²)**	26.80/34.86/35.04	24.72/35.76/34.49	27.32/40.48/37.26	22.23/36.47/32.5	17.18/24.05/28.92
Ramanchandran Favored	99.04	99.68	99.37	99.37	98.75
Ramanchandran allowed	0.96	0.32	0.63	0.63	0.94
Ramanchandran Disallowed	0	0	0	0	0.31

PDB ID:	6SZX	6SZY	6T01	6T0O	6T02
Fragment	**11**	**12**	**13**	**14**	**15**
Data Collection					
Space group	$P12_11$	$P12_11$	$P12_11$	$P12_11$	$P12_11$
Cell dimension a, b, c (Å)	39.77, 103.86, 42.02	39.38, 102.96, 41.98	39.68, 103.32, 42.25	39.47, 103.07, 41.95	39.65, 103.26, 42.43
Cell dimension α, β, γ (°)	90, 104.06, 90	90, 106.87, 90	90, 105.76, 90	90, 106.73, 90	90, 104.93, 90
Resolution (Å)	40.75 (1.17)	40.17 (1.79)	40.65 (1.5)	40.17 (1.71)	40.998 (1.1)
Unique reflections*	109553 (17058)	29267 (4584)	51239 (8245)	34549 (5527)	131033 (20349)
Completeness*	98.9 (95.7)	97.4 (95)	98.5 (98.2)	99.5 (98.7)	98.7 (95.1)
Redundancy*	3.27 (2.89)	3.5 (3.53)	3.36 (3.16)	3.38 (3.47)	3.24 (2.92)
R_{merge}*	6.5 (80.9)	11 (105.5)	10.5 (111.3)	8.4 (90.2)	5.1 (102.3)
CC (1/2)	99.9 (59.3)	99.7 (61.5)	99.8 (44.6)	99.8 (72.2)	100 (53.4)
I/σI	11.75 (1.5)	8.95 (1.52)	10.03 (1.18)	12.71 (1.69)	13.73 (1.2)
Refinement					
R_{work}/R_{free}	0.1938/0.2098	0.1841/0.2232	0.2081/0.2423	0.1865/0.2253	0.1870/0.2003
RMSD bond (Å)	0.005	0.006	0.006	0.006	0.004
RMSD angle (°)	0.767	0.853	0.991	0.82	0.83
B-factor (Å²)**	13.83/16.83/24.72	25.07/37.95/33.86	17.04/28.57/27.52	26.64/40.81/35.16	14.95/24.5/25.2
Ramanchandran Favored	99.68	98.73	99.38	99.06	99.36
Ramanchandran allowed	0.32	1.27	0.62	0.94	0.64
Ramanchandran Disallowed	0	0	0	0	0

PDB ID:	6T03	6T04	6T05	6T06	6T07
Fragment	**16**	**17**	**18**	**19**	**20**
Data Collection					
Space group	$P12_11$	$P12_11$	$P12_11$	$P12_11$	$P12_11$
Cell dimension a, b, c (Å)	39.85, 103.67, 42.55	39.76, 103.33, 42.38	39.65, 103.28, 42.32	39.37, 102.86, 42.04	39.58, 103.35, 42.20
Cell dimension α, β, γ (°)	90, 105.72, 90	90, 104.51, 90	90, 104.62, 90	90, 106.04, 90	90, 105.3, 90
Resolution (Å)	40.962 (1.5)	41.02 (1.5)	40.94 (1.5)	40.4 (2.4)	40.7 (1.5)
Unique reflections*	51687 (8259)	51596 (8293)	52153 (8220)	11567 (1687)	51510 (8071)
Completeness*	97.3 (96.5)	96.4 (95.8)	97.3 (94.8)	91.1 (82.9)	99 (96.4)
Redundancy*	3.39 (3.33)	2.57 (2.31)	3.22 (2.88)	2.99 (2.71)	3.34 (3.1)
R_{merge}*	3.1 (12.6)	2.4 (7)	4.7 (25.5)	4.1 (9.9)	6.6 (76.1)
CC (1/2)	99.9 (98.7)	99.9 (99.4)	99.8 (96.7)	99.9 (98.9)	99.8 (67.9)
I/σI	27.43 (9.89)	32.49 (13.91)	18.64 (5.58)	23.15 (9.76)	10.99 (1.59)
Refinement					
R_{work}/R_{free}	0.1739/0.1946	0.1694/0.1917	0.1859/0.2207	0.1765/0.2586	0.1869/0.2159
RMSD bond (Å)	0.006	0.005	0.005	0.008	0.006
RMSD angle (°)	0.885	0.798	0.828	0.957	0.811
B-factor (Å²)**	19.62/32.95/31.35	16.35/22.41/28.77	18.76/27.15/30.05	27.52/41.02/29.75	22.78/34.12/33.23
Ramanchandran Favored	99.37	99.03	99.03	97.75	99.03
Ramanchandran allowed	0.63	0.97	0.97	2.25	0.65
Ramanchandran Disallowed	0	0	0	0	0.32

PDB ID:	6T08	6T0X	6T0Z	6T09	6T0A
Fragment	**21**	**22**	**23**	**24**	**25**
Data Collection					
Space group	$P12_11$	$P12_11$	$P12_11$	$P12_11$	$P12_11$
Cell dimension a, b, c (Å)	39.82, 103.79, 42.05	39.56, 103.09, 42.11	39.60, 103.25, 42.11	39.67, 103.26, 42.14	39.62, 102.93, 42.05
Cell dimension α, β, γ (°)	90, 104.94, 90	90, 105.45, 90	90, 105.5, 90	90, 105.56, 90	90, 105.72, 90
Resolution (Å)	40.63 (1.41)	40.58 (1.36)	40.57 (1.43)	40.59 (1.75)	40.47 (2.02)
Unique reflections*	62630 (9986)	68687 (10862)	59461 (9532)	61712 (9458)	21180 (3401)
Completeness*	99.3 (98.3)	99.1 (97.4)	99.4 (99)	94.8 (90.2)	99.6 (99.6)
Redundancy*	3.33 (3.3)	3.39 (3.43)	3.37 (3.38)	1.75 (1.62)	3.42 (3.31)
R_{merge}*	5.7 (90.7)	6.3 (95.1)	7 (87.3)	8.5 (99)	13.9 (81)
CC (1/2)	99.9 (63.8)	99.9 (62.7)	99.9 (72.5)	99.7 (43.8)	99.5 (62.7)
I/σI	12.79 (1.52)	13.19 (1.4)	13.77 (1.65)	8.8 (0.98)	8.97 (1.72)
Refinement					
R_{work}/R_{free}	0.1903/0.2119	0.1880/0.2132	0.1931/0.212	0.1876/0.225	0.1773/0.2294
RMSD bond (Å)	0.005	0.005	0.006	0.006	0.007
RMSD angle (°)	0.755	0.882	0.857	0.879	0.867
B-factor (Å²)**	21.57/28.01/31.21	19.03/30.66/29.52	19.44/32.46/29.37	25.48/40.63/33.16	25.99/37.49/32.68
Ramanchandran Favored	99.38	99.38	98.46	99.04	98.77
Ramanchandran allowed	0.62	0.31	1.54	0.96	1.23
Ramanchandran Disallowed	0	0.31	0	0	0

PDB ID:	6T0C	6T0D	6T10	6T11	6T12
Fragment	**26**	**27**	**28**	**29**	**30**
Data Collection					
Space group	$P12_11$	$P12_11$	$P12_11$	$P12_11$	$P12_11$
Cell dimension a, b, c (Å)	39.80, 103.56, 42.11	39.97, 103.99, 42.03	39.74, 103.52, 42.19	39.74, 103.44, 42.18	39.95, 103.47, 42.47
Cell dimension α, β, γ (°)	90, 105.54, 90	90, 105.39, 90	90, 105.73, 90	90, 105.43, 90	90, 105.16, 90
Resolution (Å)	40.568 (2.03)	40.51 (1.43)	40.6 (1.48)	40.65 (1.49)	40.989 (1.46)
Unique reflections*	21045 (3238)	59103 (9114)	53460 (8464)	52660 (8126)	56952 (9152)
Completeness*	98.8 (94.9)	96.4 (92.4)	98.2 (96.4)	97.5 (93.5)	98 (97.9)
Redundancy*	3.36 (3.26)	3.52 (3.42)	3.43 (3.31)	3.43 (3.28)	3.39 (3.27)
R_{merge}*	24.1 (124)	7.7 (120.8)	6.3 (79.2)	5.3 (89.7)	3.3 (29.5)
CC (1/2)	98.2 (71.7)	99.7 (59.2)	99.9 (70.7)	99.9 (72.8)	99.9 (93.6)
I/σI	4.44 (1.1)	9.3 (0.98)	13.72 (1.64)	12.39 (1.4)	21.92 (4.13)
Refinement					
R_{work}/R_{free}	0.2163/0.2734	0.2033/0.2328	0.1899/0.2099	0.2007/0.2180	0.1755/0.1957
RMSD bond (Å)	0.007	0.005	0.006	0.008	0.005
RMSD angle (°)	0.897	0.797	0.899	0.968	0.819
B-factor (Å²)**	27.88/37.56/30.05	26.10/34.24/35.05	21.17/36.36/31.03	28.14/41.90/36.68	19.7/27.53/29.73
Ramanchandran Favored	97.47	98.07	99.04	99.06	99.05
Ramanchandran allowed	2.22	1.61	0.96	0.94	0.95
Ramanchandran Disallowed	0.31	0.32	0	0	0

*Statistics for the highest resolution shell is shown in parentheses.

** P/L/W indicate protein, ligand/ion and water molecules, respectively.

Table S2: Twenty-four of the 30 fragments were tested at a single concentration of 1 mM in the HTRF competition assay against the YTHDF1/2/3 reader domains. The percentage value is the remaining HTRF signal in the presence of the test fragments with respect to the DMSO control. Lower percentage values indicate higher affinity and values below 50% are in italics and red.

Fragments	YTHDF1 (%)	YTHDF2 (%)	YTHDF3 (%)
1	104		
2			
3			
4		79	112
5	90	94	
6		*44*	
7		103	
8	93		
9	112	66	
10	106	98	
11	132	98	
12	64	88	116
13			
14			
15		89	96
16	65	70	
17	80	99	
18	103	100	
19	85	102	
20	103	96	
21	103	89	114
22	78		
23	79	104	118
24			
25			
26	*26*	*4*	*37*
27	90	93	90
28	64	63	63
29	69	63	95
30	102	98	124

Figure S3: 2Fo-Fc electron density maps of fragments bound to YTHDC1 at a contour level of 0.8-1.0 sigma.

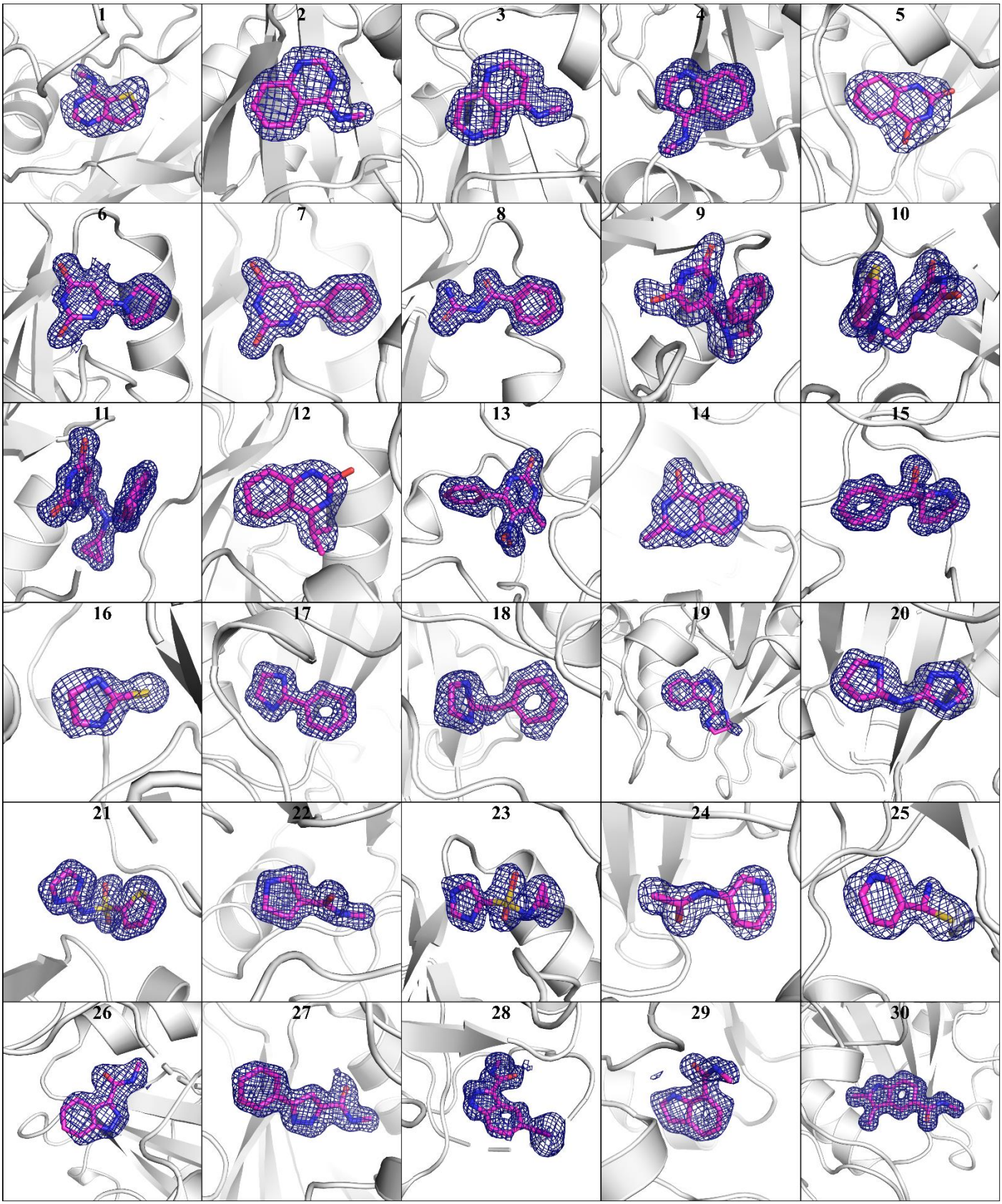

Figure S4: Crystal structures of the complexes between the m6A-reader domain of YTHDC1 (gray) and 30 fragments (carbon atoms in magenta). The binding mode of m6A (black thin lines) is shown as a basis of comparison. The conserved hydrogen bond between the main chain carbonyl of Ser378 and a hydrogen bond donor of the ligand is shown (green dashed lines). The PDB codes are listed in Table S1.

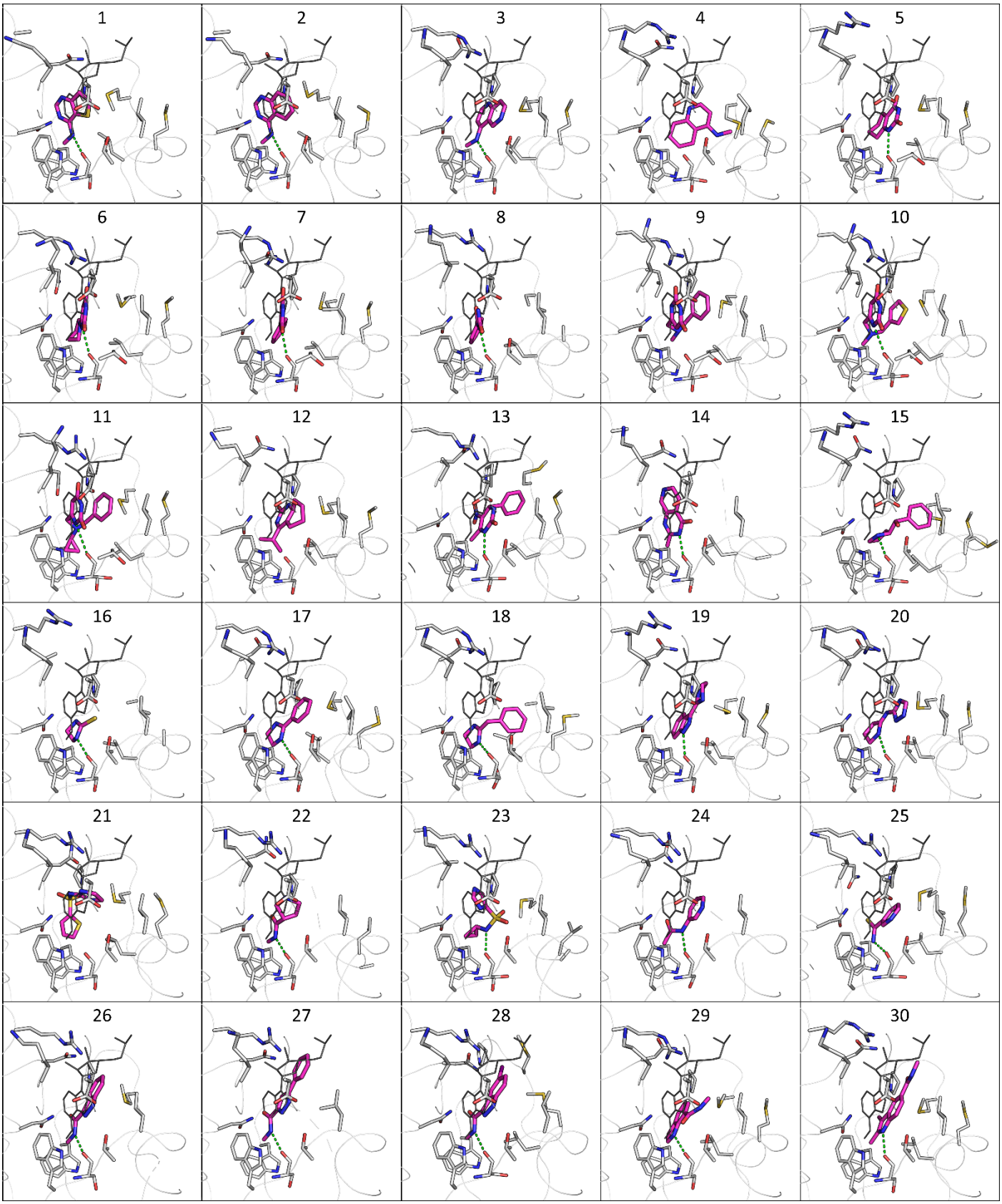

Reference

1. Li, Y.; Bedi, R. K.; Wiedmer, L.; Huang, D.; Sledz, P.; Caflisch, A., Flexible Binding of m(6)A Reader Protein YTHDC1 to Its Preferred RNA Motif. *J Chem Theory Comput* **2019,** *15* (12), 7004-7014.
2. Kabsch, W., Xds. *Acta Crystallogr D Biol Crystallogr* **2010,** *66* (Pt 2), 125-32.
3. McCoy, A. J.; Grosse-Kunstleve, R. W.; Adams, P. D.; Winn, M. D.; Storoni, L. C.; Read, R. J., Phaser crystallographic software. *J Appl Crystallogr* **2007,** *40* (Pt 4), 658-674.
4. Liebschner, D.; Afonine, P. V.; Baker, M. L.; Bunkoczi, G.; Chen, V. B.; Croll, T. I.; Hintze, B.; Hung, L. W.; Jain, S.; McCoy, A. J.; Moriarty, N. W.; Oeffner, R. D.; Poon, B. K.; Prisant, M. G.; Read, R. J.; Richardson, J. S.; Richardson, D. C.; Sammito, M. D.; Sobolev, O. V.; Stockwell, D. H.; Terwilliger, T. C.; Urzhumtsev, A. G.; Videau, L. L.; Williams, C. J.; Adams, P. D., Macromolecular structure determination using X-rays, neutrons and electrons: recent developments in Phenix. *Acta Crystallogr D Struct Biol* **2019,** *75* (Pt 10), 861-877.
5. Emsley, P.; Lohkamp, B.; Scott, W. G.; Cowtan, K., Features and development of Coot. *Acta Crystallogr D Biol Crystallogr* **2010,** *66* (Pt 4), 486-501.
6. Afonine, P. V.; Grosse-Kunstleve, R. W.; Echols, N.; Headd, J. J.; Moriarty, N. W.; Mustyakimov, M.; Terwilliger, T. C.; Urzhumtsev, A.; Zwart, P. H.; Adams, P. D., Towards automated crystallographic structure refinement with phenix.refine. *Acta Crystallogr D Biol Crystallogr* **2012,** *68* (Pt 4), 352-67.
7. Wiedmer, L.; Eberle, S. A.; Bedi, R. K.; Sledz, P.; Caflisch, A., A Reader-Based Assay for m(6)A Writers and Erasers. *Anal Chem* **2019,** *91* (4), 3078-3084.
8. Xu, C.; Wang, X.; Liu, K.; Roundtree, I. A.; Tempel, W.; Li, Y.; Lu, Z.; He, C.; Min, J., Structural basis for selective binding of m6A RNA by the YTHDC1 YTH domain. *Nat. Chem. Biol.* **2014,** *10* (11), 927-9.
9. Brooks, B. R.; Brooks, C. L.; Mackerell, A. D.; Nilsson, L.; Petrella, R. J.; Roux, B.; Won, Y.; Archontis, G.; Bartels, C.; Boresch, S.; Caflisch, A.; Caves, L.; Cui, Q.; Dinner, A. R.; Feig, M.; Fischer, S.; Gao, J.; Hodoscek, M.; Im, W.; Kuczera, K.; Lazaridis, T.; Ma, J.; Ovchinnikov, V.; Paci, E.; Pastor, R. W.; Post, C. B.; Pu, J. Z.; Schaefer, M.; Tidor, B.; Venable, R. M.; Woodcock, H. L.; Wu, X.; Yang, W.; York, D. M.; Karplus, M., CHARMM: The Biomolecular Simulation Program. *Journal of Computational Chemistry* **2009,** *30* (10), 1545-1614.
10. Jorgensen, W. L.; Chandrasekhar, J.; Madura, J. D.; Impey, R. W.; Klein, M. L., Comparison of Simple Potential Functions for Simulating Liquid Water. *Journal of Chemical Physics* **1983,** *79* (2), 926-935.
11. Huang, J.; MacKerell, A. D., CHARMM36 all-atom additive protein force field: Validation based on comparison to NMR data. *Journal of Computational Chemistry* **2013,** *34* (25), 2135-2145.
12. Phillips, J. C.; Braun, R.; Wang, W.; Gumbart, J.; Tajkhorshid, E.; Villa, E.; Chipot, C.; Skeel, R. D.; Kale, L.; Schulten, K., Scalable molecular dynamics with NAMD. *Journal of Computational Chemistry* **2005,** *26* (16), 1781-1802.
13. Martyna, G. J.; Tobias, D. J.; Klein, M. L., Constant-Pressure Molecular-Dynamics Algorithms. *Journal of Chemical Physics* **1994,** *101* (5), 4177-4189.
14. Feller, S. E.; Zhang, Y. H.; Pastor, R. W.; Brooks, B. R., Constant-Pressure Molecular-Dynamics Simulation - the Langevin Piston Method. *Journal of Chemical Physics* **1995,** *103* (11), 4613-4621.
15. Steinbach, P. J.; Brooks, B. R., New Spherical-Cutoff Methods for Long-Range Forces in Macromolecular Simulation. *Journal of Computational Chemistry* **1994,** *15* (7), 667-683.
16. Essmann, U.; Perera, L.; Berkowitz, M. L.; Darden, T.; Lee, H.; Pedersen, L. G., A Smooth Particle Mesh Ewald Method. *Journal of Chemical Physics* **1995,** *103* (19), 8577-8593.
17. Schmidtke, P.; Bidon-Chanal, A.; Luque, F. J.; Barril, X., MDpocket: open-source cavity detection and characterization on molecular dynamics trajectories. *Bioinformatics* **2011,** *27* (23), 3276-3285.
18. Le Guilloux, V.; Schmidtke, P.; Tuffery, P., Fpocket: An open source platform for ligand pocket detection. *Bmc Bioinformatics* **2009,** *10*.